

# Longitudinal and transverse right ventricular function in pulmonary hypertension: cardiovascular magnetic resonance imaging study from the ASPIRE registry

Andrew J. Swift,<sup>1,2</sup> Smitha Rajaram,<sup>1</sup> Dave Capener,<sup>1</sup> Charlie Elliot,<sup>3</sup> Robin Condliffe,<sup>3</sup> Jim M. Wild,<sup>1</sup> David G. Kiely<sup>3</sup>

<sup>1</sup>Academic Unit of Radiology, University of Sheffield, Sheffield, United Kingdom; <sup>2</sup>Institute of Insilico Medicine, University of Sheffield, Sheffield, United Kingdom; <sup>3</sup>Sheffield Pulmonary Vascular Clinic, Sheffield Teaching Hospitals Trust, Sheffield, United Kingdom

**Abstract:** Right ventricular (RV) function is a strong predictor of outcome in cardiovascular diseases. Two components of RV function, longitudinal and transverse motion, have been investigated in pulmonary hypertension (PH). However, their individual clinical significance remains uncertain. The aim of this study was to determine the factors associated with transverse and longitudinal RV motion in patients with PH. In 149 treatment-naive patients with PH and 16 patients with suspected PH found to have mean pulmonary arterial pressure of <20 mmHg, cardiovascular magnetic resonance imaging was performed within 24 hours of right heart catheterization. In patients with PH, fractional longitudinal motion (fractional tricuspid annulus to apex distance [f-TAAD]) was significantly greater than fractional transverse motion (fractional septum to free wall distance [f-SFD];  $P = 0.002$ ). In patients without PH, no significant difference between f-SFD and f-TAAD was identified ( $P = 0.442$ ). Longitudinal RV motion was singularly associated with RV ejection fraction independent of age, invasive hemodynamics, and cardiac magnetic resonance measurements ( $P = 0.024$ ). In contrast, transverse RV motion was independently associated with left ventricular eccentricity ( $P = 0.036$ ) in addition to RV ejection fraction ( $P = 0.014$ ). In conclusion, RV motion is significantly greater in the longitudinal direction in patients with PH, whereas patients without PH have equal contributions of transverse and longitudinal motion. Longitudinal RV motion is primarily associated with global RV pump function in PH. Transverse RV motion not only reflects global pump function but is independently influenced by ventricular interaction in patients with PH.

**Keywords:** pulmonary hypertension, magnetic resonance imaging, right ventricle.

*Pulm Circ* 2015;5(3):557-564. DOI: 10.1086/682428.

Right ventricular (RV) dysfunction is considered a key determinant of adverse outcomes in several cardiopulmonary disease states. RV dilatation<sup>1-3</sup> and progressive reduction in RV ejection fraction (RVEF) predicts mortality in patients with pulmonary arterial hypertension (PAH).<sup>1,3</sup> In addition, RV dysfunction predicts mortality in patients following myocardial infarction<sup>4,5</sup> and in nonischemic cardiomyopathy.<sup>6</sup>

The transverse and longitudinal components of RV function have been studied previously in patients with pulmonary hypertension (PH).<sup>7,8</sup> However, there are conflicting data regarding the importance of transverse and longitudinal shortening in relation to global RV function in PH. Longitudinal shortening measured using tricuspid annular plane systolic excursion (TAPSE) has been shown to be a strong predictor of adverse outcomes in patients with PH,<sup>9,10</sup> and it has been postulated that longitudinal motion, rather than transverse motion, is the main determinant of RVEF in both healthy subjects and patients with PH.<sup>8</sup> In direct contrast, Kind et al.<sup>7</sup> demonstrated a stronger association between trans-

verse RV motion and RVEF than between longitudinal RV motion and RVEF in patients with PH. Moreover, Mauritz et al.<sup>11</sup> identified transverse RV motion to be a stronger determinant of adverse outcomes in patients with severe PAH, with the floor effect of longitudinal motion masking end-stage RV decline. Longitudinal and transverse RV motion are both likely important markers of disease severity; however, their association with invasive hemodynamic, cardiac volumetric, and functional magnetic resonance imaging (MRI) measurements as well as their clinical significance remain unknown.

The aim of this study was to determine the covariate factors associated with transverse and longitudinal RV motion in patients with PH.

## METHODS

### Patients

Consecutive treatment-naive patients undergoing right heart catheterization (RHC) and MRI for suspected PH were identified over a

Address correspondence to Dr. Andrew J. Swift, Academic Unit of Radiology, University of Sheffield, C Floor, Royal Hallamshire Hospital, Glossop Road, Sheffield S10 2J, United Kingdom. E-mail: a.j.swift@shef.ac.uk.

Submitted October 15, 2014; Accepted March 23, 2015; Electronically published July 24, 2015.

© 2015 by the Pulmonary Vascular Research Institute. All rights reserved. 2045-8932/2015/0503-0015. \$15.00.

2-year period at a PH referral center from the ASPIRE (Assessing the Spectrum of Pulmonary Hypertension Identified at a Referral Centre) registry.<sup>12</sup> Inclusion criteria required that the patients' RHC and MRI be performed within 48 hours after admission. Patients were excluded if the imaging was of nondiagnostic quality. Approval for retrospective analysis of imaging techniques was granted by the local research ethics committee.

### MRI acquisition

MRI was performed on a 1.5-T whole-body scanner (GE HDx; GE Healthcare, Milwaukee, WI), using an 8-channel cardiac coil. Four-chamber and short-axis cine images were acquired using a cardiac gated multislice balanced steady-state free precession sequence (20 frames per cardiac cycle; slice thickness: 8 mm; field of view: 48; matrix: 256 × 256; bandwidth: 125 KHz/pixel; repetition time/echo time: 3.7/1.6 ms). A stack of images in the short-axis plane with slice thickness of 8 mm (2-mm interslice gap) were acquired fully covering both ventricles from base to apex. We corrected our MRI parameters where appropriate for body surface area (BSA), as reported elsewhere in the literature.<sup>1</sup>

### Image analysis

Image analysis was performed on a GE Advantage Workstation 4.1 by a pulmonary vascular radiologist (AJS) who was masked to patient clinical information and cardiac catheter parameters. A second observer analyzed 40 patients at random to assess interobserver agreement. Patients' scans were defined as nondiagnostic when image quality significantly affected cardiac measurements or volumetric analysis could not be accurately performed.

### RV volume and function

Endocardial surfaces were manually traced from the stack of short-axis cine images using our MRI workstation software (GE Advantage Workstation ReportCard) to obtain RV end-diastolic (RVEDV) and end-systolic (RVESV) volumes. From these, the RVEF was calculated as  $RVEF = (RVEDV - RVESV)/RVEDV$ .

Longitudinal RV motion was assessed using TAPSE, a measurement previously evaluated using echocardiography and MRI.<sup>7,9,13</sup> TAPSE was calculated manually from the change of the tricuspid annulus to apex distance between end-diastolic and end-systolic four-chamber images. Fractional measure of longitudinal motion utilized the tricuspid annulus to apex distance change (*f*-TAAD) and was calculated as TAPSE divided by the tricuspid annulus to apex dimension at end diastole expressed as a percentage. This method has been described elsewhere by Kind et al.<sup>7</sup>

Transverse RV motion was determined from the change in the septum to free wall perpendicular distance (SFD) on the four-chamber images. As described elsewhere by Kind et al.,<sup>7</sup> lines were drawn between the tricuspid annulus and the apex and between the mitral annulus and the apex. The line intersecting the midpoints of these two lines defines the transverse axis of the heart. Septum to free wall dimensions followed this intersecting line (Fig. 1). SFD was measured manually as the change between the

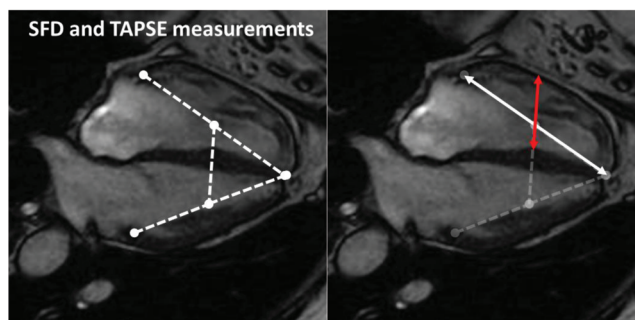


Figure 1. Four-chamber images from a patient with mild pulmonary hypertension showing tricuspid annulus to apex distance (TAAD) measurements (right image, white line) and septum to free wall distance (SFD) measurements (right image, red line).

SFD at end diastole and the SFD at end systole. Fractional SFD (*f*-SFD) was calculated as for fractional longitudinal motion.<sup>7</sup>

### Left ventricular (LV) eccentricity

LV eccentricity measurements have been traditionally expressed as the ratio of the length of two LV perpendicular minor-axis diameters. Systolic eccentricity index (sEI) measurements were obtained from the midchamber short-axis end-systolic image, and the ratio was calculated by the formula  $sEI = D2/D1$ , where D2 is the diameter parallel to the interventricular septum (IVS) and D1 is the diameter perpendicular to it. Abnormal values derived from echocardiography are considered to be >1.2.<sup>14</sup> Diastolic eccentricity index (dEI) was also calculated.

### RV mass index and ventricular mass index (VMI)

The RV epicardial and endocardial borders on each end-diastolic short-axis slice image were outlined. The IVS was considered part of the LV. The myocardial volume for each slice was calculated by multiplying the area of the RV wall by the slice thickness. The product of the sum total of the myocardial slice volumes for each ventricle and the density of myocardium ( $1.05 \text{ g/cm}^3$ ) gave an estimate of RV mass.<sup>15,16</sup> The LV epicardial and endocardial borders on each end-diastolic short-axis slice were outlined, and LV end-diastolic mass was derived as described above. VMI was defined as RV mass divided by LV mass.

### RHC, echocardiography, and clinical evaluation

RHC was performed using a balloon-tipped 7.5-Fr thermodilution catheter (Becton Dickinson, Franklin Lakes, NJ). Patients referred for the investigation of suspected PH also underwent clinical evaluation, including blood testing, echocardiography, computed tomography scanning, lung function testing, incremental shuttle walk test (ISWT), exercise testing, and perfusion lung imaging. Diagnostic classification of the form of PH was done using standard criteria following multidisciplinary assessment.<sup>17</sup> Diagnostic classification was reached in accordance with standard criteria after multidisciplinary assessment by pulmonary vascular physicians and radiologists. Diagnosis was considered to occur at the time of the first RHC showing the pres-

Table 1. Demographic, right heart catheterization, and cardiac magnetic resonance imaging (MRI) data in patients with pulmonary hypertension (PH) and in those without PH

	PH ( <i>n</i> = 149)	No PH ( <i>n</i> = 16)	<i>P</i>
Demographics			
Age, years	64 ± 14	62 ± 16	0.673
Female, % (proportion)	63 (94/149)	69 (11/16)	0.657
WHO functional class, no. (%)			
1	3 (2)	2 (5)	...
2	31 (21)	6 (38)	
3	97 (65)	8 (50)	
4	18 (12)	0 (0)	
Clinical classification, no.			
Group 1 PAH	61	NA	NA
IPAH	29		
PAH-CTD	26		
PAH-CHD	4		
Portal PAH	2		
Group 2 PAH: PH due to left heart disease	18	NA	NA
Group 3 PAH: PH due to lung diseases and/or hypoxia	22	NA	NA
Group 4 PAH: CTEPH	48	NA	NA
Invasive catheter measurements			
mRAP, mmHg	11 ± 6	5 ± 2	<0.0001
mPAP, mmHg	45 ± 13	16 ± 2	<0.0001
PCWP, mmHg	13 ± 5	9 ± 3	0.006
CI, L/min/m <sup>2</sup>	2.8 ± 0.8	3.5 ± 0.5	0.001
PVRI, WU/m <sup>2</sup>	13.2 ± 8.9	2.1 ± 0.9	<0.0001
m $\dot{V}$ O <sub>2</sub> , %	62.8 ± 9.6	73.1 ± 4.4	<0.0001
Echocardiography			
Tricuspid regurgitant jet velocity, m/s	4 ± 0.9	2.5 ± 0.6	<0.0001
MRI			
RVEDVI, mL/m <sup>2</sup>	102 ± 40	75 ± 13	0.009
VMI, ratio	0.73 ± 0.37	0.28 ± 0.1	<0.0001
RVEF, %	25.1 ± 1.9	43 ± 11	<0.0001
RVSVI, mL/m <sup>2</sup>	23.6 ± 14.2	33 ± 12	0.016
TAPSE, mm	15 ± 6.6	22 ± 5.2	<0.0001
f-TAAD, %	15.2 ± 7.3	25.5 ± 5.7	<0.0001
SFD, mm	6.0 ± 5.3	11 ± 0.5	<0.0001
f-SFD, %	13.2 ± 12.3	27.9 ± 10.1	<0.0001
sEI, ratio	1.6 ± 0.5	1.1 ± 0.1	0.001
dEI, ratio	1.3 ± 0.2	1.1 ± 0.1	0.031

Note: Except where otherwise noted, data are mean ± standard deviation. CI: cardiac index; CTEPH: chronic thrombo-embolic pulmonary hypertension; dEI: left ventricular diastolic eccentricity index; f-SFD: fractional septum to free wall distance; f-TAAD: fractional tricuspid annulus to apex distance; IPAH: idiopathic PAH; mPAP: mean pulmonary arterial pressure; mRAP: mean right atrial pressure; m $\dot{V}$ O<sub>2</sub>: mixed venous oxygen saturation; NA: not applicable; PAH: pulmonary arterial hypertension; PAH-CHD: congenital heart disease-associated PAH; PAH-CTD: connective tissue disease-associated PAH; PCWP: pulmonary capillary wedge pressure; PVRI: pulmonary vascular resistance index; RVEDVI: right ventricular end-diastolic volume index; RVEF: right ventricular ejection fraction; RVSVI: right ventricular stroke volume index; sEI: left ventricular systolic eccentricity index; SFD: septum to free wall distance; TAPSE: tricuspid annular plane systolic excursion; VMI: ventricular mass index; WHO: World Health Organization; WU: Wood units.

ence of PH. Patients with Eisenmenger syndrome, in whom RHC is not routinely required, were excluded.<sup>18</sup> Echocardiography was performed by trained cardiac physiologists using Powervision 6000 and 8000 machines (Toshiba, Tokyo, Japan) as part of routine clinical care using a standard protocol for these patients. Multiple windows were used to obtain the optimal Doppler estimation of tricuspid regurgitant jet velocity (TRJV).

### Clinical subgroup classification

To be classified as group 1 PAH, the pulmonary capillary wedge pressure (PCWP) at RHC was required to be  $\leq 15$ . Pulmonary vascular resistance (PVR) was determined as follows:  $PVR = (mPAP - PCWP)/CO$ , where mPAP is mean pulmonary arterial pressure and CO is cardiac output. Patients with familial PAH or PAH in association with drug use were considered to have idiopathic PAH; this approach has been employed previously.<sup>19</sup> Patients with PH due to left heart disease (PH-LHD; group 2) were identified on the basis of echocardiographic and MRI assessment of LV and left atrium morphology and function, valvular sufficiency, left atrium size, and presence of LV hypertrophy in addition to PCWP. Patients with significant lung disease were subclassified accordingly as group 3.<sup>20</sup> Patients were classified as having no PH if mPAP was  $< 20$  mmHg at rest.

### Statistics

Comparison of the longitudinal versus transverse RV function was made using a paired *t* test. Receiver operating analysis was used to identify optimal thresholds of f-SFD and f-TAAD for detecting low RVEF (defined as  $< 40\%$ ). Univariate analysis of longitudinal and transverse motion on all variables of interest was performed in all patients using the Pearson correlation coefficient. Multiple linear regression was used to test longitudinal motion (f-TAAD) and transverse motion (f-SFD) on the variables found to be significant (at the  $P < 0.05$  level) in the univariate analysis. In addition, subgroup analysis of the major PH subtypes (PAH, PH-LHD, PH associated with respiratory disease [PH-RESP], and chronic thromboembolic pulmonary hypertension [CTEPH]) was performed. Differences with a *P* value of  $< 0.05$  were considered statistically significant. To perform and display the statistics, SPSS (ver. 18; SPSS, Chicago, IL) and GraphPad Prism (ver. 5.03; GraphPad Software, San Diego, CA) were used.

### RESULTS

A total of 165 patients with suspected PH were identified, including 149 patients with PH, and 16 patients without PH (mPAP of  $< 20$  mmHg) were also included. Echocardiographic results were available for 125 patients with PH, and ISWT results were available for 134 patients. Clinical classifications, demographics, invasive hemodynamic results, and cardiac MRI results are presented in Table 1.

### Comparison of longitudinal and transverse motion

In patients with PH, longitudinal RV measurements (TAPSE) were significantly greater than transverse motion (SFD) measurements;

the mean difference was 9.4 mm (95% confidence interval: 8.4–1.0 mm;  $P < 0.0001$ ). In addition, fractional longitudinal measurements (f-TAAD) were significantly greater than fractional transverse measurements (f-SFD), with a mean difference of 2% (95% confidence interval: 0.3%–3.8%;  $P = 0.002$ ). In patients without PH (mPAP of  $< 25$  mmHg), no significant difference between f-SFD and f-TAAD was identified ( $P = 0.224$ ; Fig. 2). f-TAAD was greater than f-SFD in patients with PAH (mean difference: 4% [95% confidence interval: 1.1%–7.1%];  $P = 0.008$ ) and in patients with CTEPH (mean difference: 3% [95% confidence interval: 0.1%–5.3%];  $P = 0.048$ ). No significant difference between f-TAAD and f-SFD was found in patients with PH-LHD ( $P = 0.379$ ) and in patients with PH-RESP ( $P = 0.702$ ).

f-TAAD was significantly lower in men than in women ( $13\% \pm 5\%$  vs.  $17\% \pm 8\%$ ;  $P = 0.004$ ). Mean f-SFD was also lower in men than in women ( $11\% \pm 10\%$  vs.  $14\% \pm 14\%$ ); however, this difference was not statistically significant ( $P = 0.159$ ). f-SFD and f-TAAD were significantly higher in patients with higher World Health Organization (WHO) functional class status (3 and 4) than in those with lower WHO functional class status (1 and 2;  $P = 0.050$  and  $0.011$ , respectively).

Table 2. Correlations between transverse and longitudinal right ventricular motion parameters and covariate indexes in patients with pulmonary hypertension

	f-SFD		f-TAAD	
	<i>r</i>	<i>P</i>	<i>r</i>	<i>P</i>
Age	0.24	0.003	0.06	0.438
BSA	−0.20	0.804	0.019	0.820
mRAP	−0.06	0.149	−0.16	0.055
mPAP	−0.51	$< 0.0001$	−0.48	$< 0.0001$
PCWP	0.31	$< 0.0001$	0.23	$< 0.0001$
PVRI	−0.47	$< 0.0001$	−0.50	$< 0.0001$
CI	0.26	0.002	0.38	$< 0.0001$
$m\dot{V}O_2$	0.18	0.027	0.32	$< 0.0001$
Echo (TRJV)	−0.38	$< 0.0001$	−0.38	$< 0.0001$
RVEDVI	−0.41	$< 0.0001$	−0.38	$< 0.0001$
VMI	−0.50	$< 0.0001$	−0.51	$< 0.0001$
RVEF	−0.43	$< 0.0001$	−0.43	$< 0.0001$
sEI	−0.53	$< 0.0001$	−0.44	$< 0.0001$

Note: BSA: body surface area; f-SFD: fractional septum to free wall distance; f-TAAD: fractional tricuspid annulus to apex distance; mPAP: mean pulmonary arterial pressure; mRAP: mean right atrial pressure;  $m\dot{V}O_2$ : mixed venous oxygen saturation; PCWP: pulmonary capillary wedge pressure; PVRI: pulmonary vascular resistance index; RVEDVI: right ventricular end-diastolic volume index; RVEF: right ventricular ejection fraction; sEI: left ventricular systolic eccentricity index; TRJV: tricuspid regurgitant jet velocity; VMI: ventricular mass index.

Table 3. Multiple linear regression of longitudinal right ventricular function (fractional tricuspid annulus to apex distance) on covariate indexes

Model	Regression coefficient	SE	R <sup>2</sup>	T	P
Constant	23.433	7.817	...	2.998	0.003
mPAP	-0.069	0.115	-0.130	-0.602	0.548
CI	-0.640	1.241	-0.069	-0.515	0.607
PVRI	-0.004	0.196	-0.005	-0.019	0.985
m $\dot{V}O_2$	0.043	0.089	0.056	0.481	0.631
TRJV	-1.073	0.879	-0.129	-1.221	0.225
RVEDVI	-0.032	0.018	-0.180	-1.761	0.081
RVEF	0.125	0.048	0.242	2.630	0.010
VMI	-3.094	2.895	-0.158	-1.069	0.288
sEI	0.201	1.700	0.015	0.118	0.906

Note: CI: cardiac index; mPAP: mean pulmonary arterial pressure; m $\dot{V}O_2$ : mixed venous oxygen saturation; PVRI: pulmonary vascular resistance index; RVEDVI: right ventricular end-diastolic volume index; RVEF: right ventricular ejection fraction; sEI: left ventricular systolic eccentricity index; TRJV: tricuspid regurgitant jet velocity; VMI: ventricular mass index.

f-SFD (area under the curve [AUC]: 0.79) and f-TAAD (AUC: 0.83) showed similar accuracy for the detection of low RVEF (<40%), whereas SFD and TAPSE were less accurate for the detection of low RVEF (AUC: 0.67 and 0.76, respectively).

**Univariate regression analysis**

In univariate analysis, transverse motion as assessed by f-SFD was associated (*P* < 0.05) with patient age, mPAP, PCWP, PVR index (PVRI), cardiac index (CI), mixed  $\dot{V}O_2$ , TRJV, RVEDV index (RVEDVI), RVEF, sEI, dEI, and VMI. However, there was no association between f-SFD and mRAP (*P* = 0.149), ISWT (*P* = 0.634), or BSA (*P* = 0.804). f-TAAD was significantly associated (*P* < 0.005) with mPAP, PCWP, PVRI, CI, mixed  $\dot{V}O_2$ , RVEDVI, RVEF, sEI, dEI, and VMI. No significant associations between f-TAAD and age (*P* = 0.438), mRAP (*P* = 0.055), ISWT (*P* = 0.468), or BSA (*P* = 0.820) were found (Table 2).

In patients without PH, f-SFD and f-TAAD were associated only with RVEF (*r* = 0.40 and 0.38 [*P* < 0.05], respectively). There was no association with patient age, mPAP, PCWP, PVRI, CI, mixed  $\dot{V}O_2$ , TRJV, RVEDVI, RVEF, sEI, dEI, or VMI.

**Multivariate regression analysis**

After multiple linear regression modeling of transverse motion (f-SFD) with significant covariates, RVEF (*R*<sup>2</sup> = 0.323, *P* = 0.002) and sEI (*R*<sup>2</sup> = 0.275, *P* = 0.036) were the independent factors most closely associated with f-SFD (Fig. 3). These associations were independent of age, mPAP, PCWP, PVRI, CI, mixed  $\dot{V}O_2$ , VMI, RVEDVI,

and echocardiography-derived TRJV. Figure 3 presents a scatterplot of the associations between f-SFD on sEI and RVEDVI.

In multivariate analysis of longitudinal motion (f-TAAD) versus significant covariates, f-TAAD was significantly associated with RVEF (*R*<sup>2</sup> = 0.263, *P* = 0.010). This association was independent of all other variables in the model, namely, mPAP, PCWP, PVRI, CI, mixed  $\dot{V}O_2$ , RVEDVI, VMI, sEI, and echocardiography-derived TRJV (see Tables 3, 4).

In subgroup analysis, sEI was the only variable independently linked to f-SFD in patents with PAH (*P* < 0.0001). f-TAAD was independently associated with both RVEF (*P* = 0.013) and mPAP (*P* < 0.0001). No association between longitudinal and transverse motion was found in multivariate regression in patients with PH-LHD. In patients with PH-RESP, f-SFD was independently linked to sEI (*P* = 0.042) and there was a borderline association with RVEDVI (*P* = 0.093), whereas f-TAAD was linked to RVEF only (*P* = 0.041). In patients with CTEPH, f-SFD was independently associated with sEI (*P* = 0.006) and RVEF (*P* = 0.043).

**Reproducibility**

Good reproducibility of SFD measurements was identified (bias: 0.01 cm; SD: 0.38), with limits of agreement of -0.7 to 0.7 cm. TAPSE measurements were similarly reproducible: the bias for TAPSE measurements was 0.1 cm (SD: 0.37), with narrow limits of agreement of -0.8 to 0.6 cm.

**DISCUSSION**

This study has shown that the association between RV longitudinal motion and ejection fraction is independent of demographic, hemodynamic, and cardiac MRI indexes in PH. In contrast, RV trans-

Table 4. Multiple linear regression of transverse right ventricular function (fractional septum to free wall distance) on covariate indexes

Model	Regression coefficient	SE	R <sup>2</sup>	T	P
Constant	54.150	14.366	...	3.769	<0.0001
mPAP	-0.101	0.186	-0.114	-0.541	0.590
CI	-2.170	2.038	-0.141	-1.065	0.289
PVRI	-0.370	0.320	-0.275	-1.159	0.249
m $\dot{V}O_2$	-0.284	0.144	-0.221	-1.968	0.052
TRJV	0.259	1.512	0.019	0.171	0.864
RVEDVI	-0.052	0.029	-0.178	-1.801	0.075
RVEF	0.249	0.077	0.290	3.227	0.002
VMI	1.857	4.657	0.057	0.399	0.691
sEI	-0.592	2.790	-0.275	-2.130	0.036

Note: CI: cardiac index; mPAP: mean pulmonary arterial pressure; m $\dot{V}O_2$ : mixed venous oxygen saturation; PVRI: pulmonary vascular resistance index; RVEDVI: right ventricular end-diastolic volume index; RVEF: right ventricular ejection fraction; sEI: left ventricular systolic eccentricity index; TRJV: tricuspid regurgitant jet velocity; VMI: ventricular mass index.

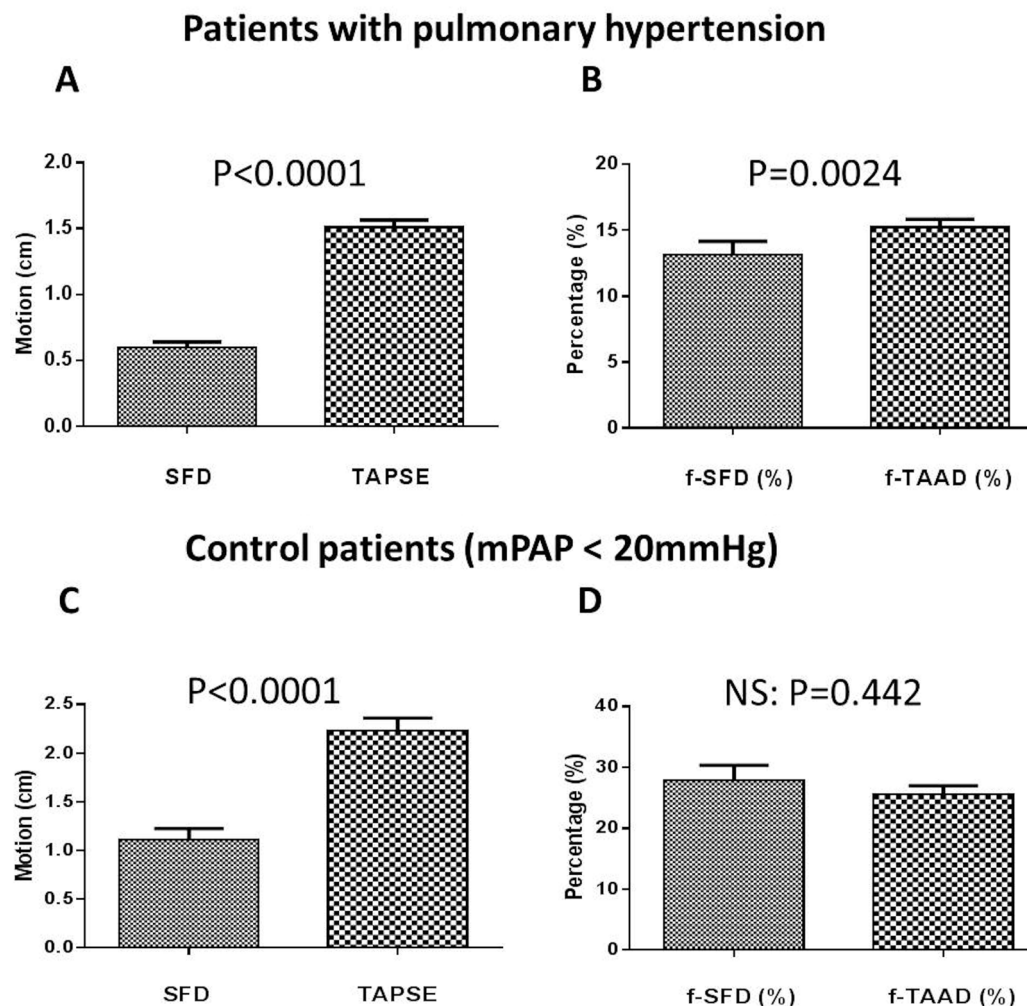


Figure 2. Comparison of transverse and longitudinal motion in patients with pulmonary hypertension (PH; *A, B*) and in those without PH (*C, D*). Absolute longitudinal motion (tricuspid annular plane systolic excursion [TAPSE]) was greater than transverse motion (septum to free wall distance [SFD]) in both patients with PH (*A*) and those without PH (*C*). Fractional longitudinal shortening (fractional tricuspid annulus to apex distance [f-TAAD]) was significantly greater than fractional transverse shortening (f-SFD) in patients with PH (*B*), whereas no significant difference was shown between f-TAAD and f-SFD in control patients (*D*). NS: not significant.

verse motion is independently influenced by ventricular interaction measured by LV eccentricity and therefore is not solely associated with RVEF.

Brown et al.<sup>8</sup> have demonstrated that in healthy subjects longitudinal motion contributes approximately 80% of global RV function. In patients with PAH, selective recovery of longitudinal rather than transverse RV function was demonstrated with therapy. The authors concluded that longitudinal function is a more important contributor to ejection fraction than transverse function in PAH. Our study has also shown that in patients with PAH and CTEPH the magnitude of RV motion is significantly greater in the longitudinal direction than in the transverse direction, whereas the RV of patients without PH (mPAP of <20 mmHg) functions with equal contributions of transverse and longitudinal motion. Patients with PH-LHD and PH-RESP also had no difference in longitudinal and transverse motion. Patient numbers were smallest in these two groups, and thus failure to find significance may be the result of

type II error. In addition, patients with PH-LHD do not tend to exhibit septal deviation as greatly,<sup>16</sup> as the pressure on the left side tends to be higher than that on the right throughout the cardiac cycle. In patients with PAH, PH-RESP, and CTEPH, transverse motion is independently linked to LV eccentricity; however, the same trend did not exist in patients with PH-LHD, similarly reflecting the lack of septal deviation in PH-LHD. Kind et al.<sup>7</sup> found that global RV function was more strongly associated with transverse RV motion than longitudinal RV motion in patients with PAH. The authors concluded that transverse RV motion may be a superior marker of RV dysfunction in PH.

The present study is the first to investigate transverse and longitudinal RV motion in terms of their associations with hemodynamic and cardiovascular MRI measurements. The findings demonstrate that both longitudinal and transverse RV motion measurements are independently associated with global RV function as measured by cardiovascular magnetic resonance-derived ejection fraction. The re-

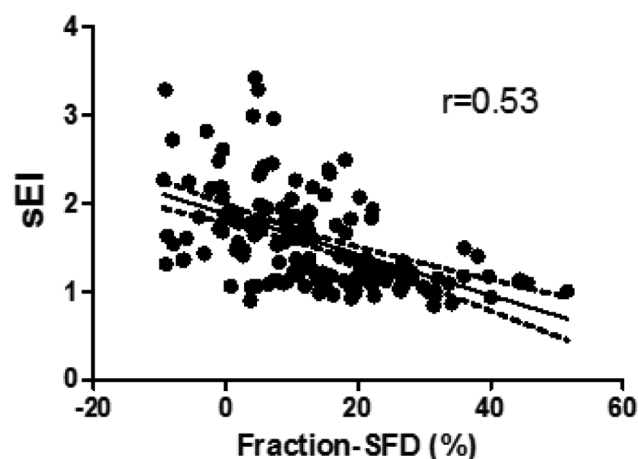


Figure 3. Scatterplot showing the association between fractional septum to free wall distance (SFD) and independent-covariates systolic eccentricity index (sEI).

relationship between longitudinal motion and global RV function is independent of all hemodynamic and imaging covariates. However, transverse RV motion is independently influenced by sEI, which is a measure of the effect of interventricular septal deviation on the LV. Patients without PH (mPAP of <20 mmHg) did not exhibit this trend. Both longitudinal and transverse motions were independently associated with global RV function, with no significant covariates identified. A recent echocardiography study has shown that, in patients with PH, reduced transverse RV function is a reliable indicator of the presence of high pulmonary arterial pressure, which is reflected in our data as transverse function and is influenced by LV eccentricity, a marker of disease severity in PH.<sup>21</sup> Second, the authors found, as we do in the present study, that reduced RV longitudinal function is more closely linked with impairment of cardiac function.<sup>21</sup> Mauritz et al.<sup>11</sup> showed that changes in transverse RV motion in severe PH were associated with increased risk of adverse outcomes. The authors suggested that a decline in transverse motion reflects progressive paradoxical interventricular motion in the later stages of the disease course. These findings are consistent with those of the present study, in which an independent association between LV eccentricity and transverse motion has been identified, and with those of previous studies showing the prognostic significance of LV eccentricity.<sup>10,22</sup>

### Limitations

This was a single-center study. Technical limitations include difficulties defining the endocardium of the RV, and due to complex trabeculations of the free wall inaccuracies may occur in the measurement of SFD. Furthermore, transverse and longitudinal motion were measured manually from four-chamber images, which may not be fully representative of their relative contributions to RVEF. Modeling the contributions of transverse and longitudinal motion using isotropic three-dimensional imaging may improve accuracy.

### Conclusions

The magnitude of RV motion is significantly greater in the longitudinal direction in patients with PH, whereas patients without PH

have equal contributions of transverse and longitudinal motion. Longitudinal and transverse components of RV function are independently linked to global RV pump function measured by RVEF. However, transverse RV motion not only reflects global pump function but is independently influenced by ventricular interaction in PH.

### ACKNOWLEDGMENTS

This article presents independent research funded by the NIHR. The views expressed are those of the authors and are not necessarily those of the National Health Service, the NIHR, or the Department of Health. JMW is also funded by the Engineering and Physical Sciences Research Council.

**Source of Support:** AJS, RC, CE, JMW, and DGK have received funding from the National Institute for Health Research (NIHR). This work was funded in part by the NIHR.

**Conflict of Interest:** DC receives funding from Bayer Schering. All other authors: none declared.

### REFERENCES

1. van Wolferen SA, Marcus JT, Boonstra A, et al. Prognostic value of right ventricular mass, volume, and function in idiopathic pulmonary arterial hypertension. *Eur Heart J* 2007;28:1250–1257.
2. Swift AJ, Rajaram S, Campbell MJ, et al. Prognostic value of cardiovascular magnetic resonance imaging measurements corrected for age and sex in idiopathic pulmonary arterial hypertension. *Circ Cardiovasc Imaging* 2014;7:100–106.
3. van de Veerdonk MC, Kind T, Marcus JT, et al. Progressive right ventricular dysfunction in patients with pulmonary arterial hypertension responding to therapy. *J Am Coll Cardiol* 2011;58:2511–2519.
4. Mehta SR, Eikelboom JW, Natarajan MK, et al. Impact of right ventricular involvement on mortality and morbidity in patients with inferior myocardial infarction. *J Am Coll Cardiol* 2001;37:37–43.
5. Zornoff LA, Skali H, Pfeffer MA, et al. Right ventricular dysfunction and risk of heart failure and mortality after myocardial infarction. *J Am Coll Cardiol* 2002;39:1450–1455.
6. Mendes LA, Dec GW, Picard MH, Palacios IF, Newell J, Davidoff R. Right ventricular dysfunction: an independent predictor of adverse outcome in patients with myocarditis. *Am Heart J* 1994;128:301–307.
7. Kind T, Mauritz GJ, Marcus JT, van de Veerdonk M, Westerhof N, Vonk-Noordegraaf A. Right ventricular ejection fraction is better reflected by transverse rather than longitudinal wall motion in pulmonary hypertension. *J Cardiovasc Magn Reson* 2010;12:35.
8. Brown SB, Raina A, Katz D, Szerlip M, Wiegers SE, Forfia PR. Longitudinal shortening accounts for the majority of right ventricular contraction and improves after pulmonary vasodilator therapy in normal subjects and patients with pulmonary arterial hypertension. *Chest* 2011;140:27–33.
9. Forfia PR, Fisher MR, Mathai SC, et al. Tricuspid annular displacement predicts survival in pulmonary hypertension. *Am J Respir Crit Care Med* 2006;174:1034–1041.
10. Ghio S, Klersy C, Magrini G, et al. Prognostic relevance of the echocardiographic assessment of right ventricular function in patients with idiopathic pulmonary arterial hypertension. *Int J Cardiol* 2010;140:272–278.
11. Mauritz GJ, Kind T, Marcus JT, et al. Progressive changes in right ventricular geometric shortening and long-term survival in pulmonary arterial hypertension. *Chest* 2012;141:935–943.
12. Hurdman J, Condliffe R, Elliot CA, et al. ASPIRE registry: assessing the Spectrum of Pulmonary hypertension Identified at a REFerral centre. *Eur Respir J* 2012;39:945–955.

13. Gupta S, Khan F, Shapiro M, Weeks SG, Litwin SE, Michaels AD. The associations between tricuspid annular plane systolic excursion (TAPSE), ventricular dyssynchrony, and ventricular interaction in heart failure patients. *Eur J Echocardiogr* 2008;9:766–771.
14. Lopez-Candales A, Rajagopalan N, Kochar M, Gulyasy B, Edelman K. Systolic eccentricity index identifies right ventricular dysfunction in pulmonary hypertension. *Int J Cardiol* 2008;129:424–426.
15. Hagger D, Condliffe R, Woodhouse N, et al. Ventricular mass index correlates with pulmonary artery pressure and predicts survival in suspected systemic sclerosis-associated pulmonary arterial hypertension. *Rheumatology* 2009;48:1137–1142.
16. Swift AJ, Rajaram S, Condliffe R, et al. Diagnostic accuracy of cardiovascular magnetic resonance imaging of right ventricular morphology and function in the assessment of suspected pulmonary hypertension results from the ASPIRE registry. *J Cardiovasc Magn Reson* 2012;14:40.
17. Galiè N, Hoeper MM, Humbert M, et al. Guidelines for the diagnosis and treatment of pulmonary hypertension. *Eur Respir J* 2009;34:1219–1263.
18. Dimopoulos K, Inuzuka R, Goletto S, et al. Improved survival among patients with Eisenmenger syndrome receiving advanced therapy for pulmonary arterial hypertension. *Circulation* 2010;121:20–25.
19. Kawut SM, Horn EM, Berekashvili KK, et al. New predictors of outcome in idiopathic pulmonary arterial hypertension. *Am J Cardiol* 2005;95:199–203.
20. Chaouat A, Naeije R, Weitzenblum E. Pulmonary hypertension in COPD. *Eur Respir J* 2008;32:1371–1385.
21. Pica S, Ghio S, Tonti G, et al. Analyses of longitudinal and of transverse right ventricular function provide different clinical information in patients with pulmonary hypertension. *Ultrasound Med Biol* 2014;40:1096–1103.
22. Raymond RJ, Hinderliter AL, Willis PW, et al. Echocardiographic predictors of adverse outcomes in primary pulmonary hypertension. *J Am Coll Cardiol* 2002;39:1214–1219.